RSC Advances

ROYAL SOCIETY OF CHEMISTRY

www.rsc.org/advances

Journal Name

RSCPublishing

ARTICLE

Core double-shell cobalt/graphene/polystyrene magnetic nanocomposites synthesized by *in situ* sonochemical polymerization

Cite this: DOI: 10.1039/xoxxoooooox

Received ooth January 2012,
Accepted ooth January 2012

DOI: 10.1039/xoxxoooooox

www.rsc.org/

V. Hermán[a], H. Takacs[a, b], F. Duclairoir[c], O. Renault[a], J.H. Tortai[c] B. Viala[a]

Core double-shell cobalt/graphene//polystyrene nanocomposites (Co/C//PS) were synthesized by *in situ* sonochemical polymerization technique. Commercial Co/C nanoparticles are used and successfully lead to gram-scale production of processable nanocomposite. Synthesized Co/C//PS nanocomposites result in homogeneous and dense dispersion of particles with or without additional polymeric matrix. They showed improved thermal properties such as higher initial degradation temperatures and a significant increase of glass transition temperature (*i.e.* 10 to 12°C) in contrast to neat PS. These results suggest that covalent bonding occurs between PS and graphene shell, and may be promoted by two surface reactions: "grafting from" when monomer is pre-immobilized on graphene and grows to polymer, and "grafting to" when pre-synthesized polymer is immobilized on graphene. Both mechanisms are compared and explained. HR-TEM observations revealed polymer shells of 4 to 5 nm covering Co/C nanoparticles or at least small aggregates. However, the number of layer of the graphene shell which consists of 6 to 8 regular layers on raw particles decreases to 3, this layer reduction can be explained by a partial amorphization of graphene occurring during the polymerization. Nevertheless, Co particles are still efficiently protected from oxidation as final Co/C//PS nanocomposites are able to sustain high mass-magnetization (i.e. ~ 49 emu/g for 94 % wt Co/C). First indications of satisfying mechanical cohesion are also shown by the formation of two relevant nanocomposites shapes (film and disk). In conclusion, *in situ* polymerization is a powerful synthesis method to produce processable high-magnetization nanocomposites.

Introduction

3d transition-metal (Co, Ni, Fe) nanoparticles are of great importance for applications as they are expected to show elevated net moment close to those of the bulk.[1] High magnetization is a ubiquitous prerequisite for performance for many applications as it determines mechanical and dragging forces, power for magnets, permeability for electromagnetism, data storage capacity, and spin-dependent electronic transport, etc. However, beyond their successful synthesis in laboratories, their storage, manipulation, processability, and reliability remain decisive issues. The correlation between nanoparticles size, volume fraction, and magnetic properties formalize a classification of nanostructured magnetic materials with regards to their morphologies.[2] Types-A and B (*i.e.* non-interacting nanoparticles) are best represented by ferrofluids, and are generally obtained with low volume fraction of nanoparticles (*i.e.* < 10 vol. %). Type-A is based on the use of surfactant coating to prevent agglomeration with steric repulsion. Type-B uses core-shell structure mainly to stabilize colloids. In contrast, type-C and D are solid materials with high volume fraction. They consist of dense nanoparticles dispersion in a matrix. Type-C is most represented by polymer nanocomposites with volume fraction up to ~ 20 vol. %. Type-D corresponds to material with extreme volume fraction ~ 50 vol. % in reference to nanogranular or nanocrystalline solid-state materials.[2]

Self-assembly of magnetic nanoparticles (*i.e.* by precipitation on template) was reported many times,[1] but the final material is not easy to process due to poor mechanical cohesion. Conversely, when magnetic nanoparticles are embedded into a supporting polymeric matrix, the composite has good mechanical resistance and as consequence is a processable material. However, surface interactions between magnetic metallic nanoparticles and polymer matrix often lead to significant loss of net moment due to surface oxidization (*i.e.* magnetic metal oxides are ferromagnetic or antiferromagnetic)[2] or surface spin-quenching (*i.e.* with carbonyl groups mainly).[3]

Therefore the ideal processable magnetic nanocomposite for applications would consist in a polymeric dense assembly of nanoparticles with preserved high net moment and with mechanical cohesion. To achieve this requirement it is necessary to efficiently protect nanoparticles surface. In order to provide a protective shell to these systems and retain their intrinsic properties, nanoparticles have been coated with organic molecules (*i.e.* phosphine, oleic acid, and active thiol groups)[4, 5] but this method used a thin cobalt oxide layer, leading to a low magnetization. However, non-reactive materials have been used as protecting shell, such as graphite,[6] carbon/silica[7] or polymers,[8-10] and more recently graphene sheets; [11, 12] without need introducing a cobalt oxide layer.

In the field of magnetic core/shell systems for bio applications, work of R. Grass *et al.* [11, 12] was pioneer using a graphene shell as a protective layer for pure metallic cobalt nanoparticles. The flame spray technique employed by Grass *et al.*[12] enabled a production of gram scale magnetic core-shell Co/graphene (Co/C) nanoparticles which later lead to commercial production. Synthesis of Fe, Co, and Ni nanoparticles with a CVD-formed carbon shell unreactive towards a biological media has also been reported.[13] However, retaining high net-moment with carbon coated is only achieved with Co/C because carbon is very few soluble in cobalt in contrast to iron. This graphene shell not only act as protecting shell but also allows performing different types of surface chemistries, such as standard carbonaceous material functionalization routes[14] as well as polymers synthesis thanks to carbon-like chemical affinity.[15, 16]

Today there is a new challenge for magnetism community beyond bio applications which is to be able to convert such interesting powder materials (*i.e.* Co/C) into a processable material (*i.e.* Type B+C) with high mechanical resistance and high ultimate magnetization. Different processing methods with powders exist but usually refer to high temperature sintering techniques, including sol-gel method for coatings and films, that are well-suited for metal oxides nanoparticles (*i.e.* ferrites) or noble metals only (*i.e.* gold or silver).[17, 18] More recently, low curing temperature printing techniques have been developed for flexible electronics mainly, but also for polymer nanocomposite formation.[19] Printing with cobalt nanoparticles (28 nm) has been reported, but this process implies oxygen passivation of nanoparticles. As a consequence magnetic properties are degraded.[19]

The motivation of this work is to produce polymer-based nanocomposites of Co/C with high magnetic properties but not conductive. To achieve this composite we propose the use of cobalt nanoparticles covered with graphene layers that not only protect cobalt from oxidation - targeting films with high magnetization -, but also allows to perform different types of chemistries on the nanoparticles surface, such as, polymer synthesis.

Polymer-based nanocomposites are of interest for many low cost applications as they are well-suited for polymer processing technology featuring a low process temperature (molding, isostatic pressing, deep and spin coating, low curing temperature printing, etc.). However, classical polymer nanocomposites synthesis usually consists in a simple mix of nanoparticles with the polymer. This technique is not able to avoid massive nanoparticles agglomeration and results in a material extremely heterogeneous with low physical properties and poor or no mechanical cohesion. An alternative technique used to synthesize polymer nanocomposites with a good nanoparticle dispersion consists on performing *in situ* polymerization (*i.e.* carrying out polymer synthesis in the nanoparticles presences).[20]

Here, we propose the synthesis of a polymer shell superimposed on Co/C nanoparticles by *in situ* radical polymerization (*i.e.* sonochemical), leading to the novel core double-shell Co/C//Polymer (*i.e.* // means covalent grafted).[8, 21] Co/C nanoparticles were used as the key magnetic component (*i.e.* high moment). The second key component is the polymer. One suitable polymer for hybridization with graphene shell on Co/C nanoparticles is polystyrene (PS) because it presents similar sp^2 carbon atoms structure present on nanoparticles surface. Thus, it has been demonstrated that polystyrene can develop π-π interactions or covalent bonding with graphene according to [22, 23] resulting into a good mechanical cohesion.[24] Such nanocomposites were successfully synthesized by *in situ* sonochemical polymerization process. Sonochemistry is commonly used for nanoparticles dispersion and also for radical generation that are involved in PS polymerization.[25-29] To go further, sonochemical polymerization was preferred among other polymerization techniques that had also been reported for graphene sheets functionalization,[15, 26, 30-32] because the use of a sonotrode during the synthesis allows maintaining stable dispersions without using a magnetic stirrer not adapted to magnetic materials. Synthesis was performed employing different nanoparticles addition times. First, we used the statistical growth of styrene monomers being initially attached to the graphene shell on the nanoparticles (*i.e.* grafting from: adding Co/C at 0 min). Then, it is compared to the immobilization of pre-formed polystyrene chains that binds to the graphene shell when the nanoparticles are introduced after a certain time (*i.e.* grafting to: adding Co/C at 15 min).[33] Both methods are discussed here. Co/C//PS nanocomposites were systematically characterized by transmission electronic microscopy (TEM), thermal gravimetric analysis (TGA), differential scanning calorimetric (DSC), Raman, and XPS spectroscopies. Such characterizations also allowed establishing that despite a completely different nanosphere-like morphology of graphene shell, it is as reactive as flat graphene layers.[23] The mass-magnetization of Co/C//PS nanocomposites was measured with vibrating sample magnetometer (VSM) and compared to reference samples (*i.e.* raw and sonicated Co/C nanoparticles). Finally, the results were put into perspective with data reported in the literature. They showed the relevance of the sonochemical approach for Co/C based magnetic polymer nanocomposites synthesis retaining remarkable high residual net-moment at the end. Thin films were deposited by spin coating on silicon wafer or a small disk obtained by simple

compaction in a mold. They both exhibit a well-cohesive, dense, and uniform structure that is encouraging to pursue.

Experimental

Materials

This work was performed using commercial carbon-coated cobalt nanopowders (Sigma-Aldrich) with an average particle size of 30 nm. The solvents used for the synthesis are toluene as dispersing solvent (Sigma-Aldrich 99.8%), methanol as precipitating solvent (Sigma-Aldrich 99.8%), and chloroform as solubilization solvent (Sigma-Aldrich 99.8%). The reagents used are styrene (Sigma-Aldrich ≥ 99%) and 2,2′-Azobis(2-methylpropionitrile) (AIBN, Fluka, ≥ 98%).

Sonication-assisted dispersion

Prior to be used, as received nanopowders were solvent-dispersed by sonication. For this purpose, commercial Co/C nanoparticles were suspended in toluene (100 mg/10 mL) and sonicated at two different sonication powers 100 or 250 W during 30 and 15 min, respectively. The sonotrode used for these experiments is a VCX 500 Ultrasonic Processor from SONICS (500 W, 20 KHz).

PS *in situ* polymerization

The polymerization was carried out in a homemade reactor of 50 mL with three necks, one for N_2 inlet and thermometer, one for the sonotrode and the other for reagent injection (Figure 1A).

The starting solution consisted of 30 mL of a deoxygenated mixture of styrene and toluene with a volume ratio of 1:2, and 200 mg of AIBN (corresponding to 2 % of monomer weight). Sonochemical polymerization was carried out under N_2 at 100 W during 30 min (see the "Results and discussion" section). Reaction temperature is stabilized at 84 ± 2°C. Raw PS was precipitated in methanol. Then, the obtained polymer precipitate was dissolved in a minimal amount of toluene and precipitated again in methanol. This process was repeated at least four times to remove possible residual reaction products (like monomer and unreacted initiator). The final precipitated PS powder was dried under vacuum for further physicochemical analysis. PS synthesis was carried out at least three times to achieve reproducibility yield with an error ≤ 1 %.

Co/C//PS nanocomposites *in situ* polymerization

Co/C//PS nanocomposites synthesis was carried out following two different paths: 1) "Grafting from", by adding Co/C nanoparticles at the beginning of the reaction (t = 0 min) and 2) "Grafting to" by adding nanoparticles at 15 min after starting the polymerization reaction. In both cases, 100 mg of Co/C nanoparticles were dispersed in ~1 mL of toluene using an ultrasound bath. Then, the nanoparticles were introduced at the corresponding reaction times (t = 0 or 15 min) into 30 mL of a deoxygenated mixture of styrene and toluene (1:2 volume ratio) containing 200 mg of AIBN. Sonochemical *in situ* polymerization process was performed at 100 W for 30 min at 84 ± 2°C. Note that the same process described for PS synthesis was applied to obtain dry precipitated powder of Co/C//PS for physicochemical analysis. The typical quantity of final product is 1.0 to 1.5 g which is suitable for powder analysis methods and further compatible with thin-film spin-coating.

Nanocomposites synthesized were further purified (*i.e.* removing free-PS) by strong agitation in chloroform followed by centrifugation (12 x 10^3 rpm for 10min). The supernatant was discarded (free PS) and this cycle was repeated at least four times to remove all polystyrene not covalently grafted on the nanoparticle surface, in order to quantify the amount of polymer covalently grafted. Chloroform is an appropriate solvent for PS solubilization and is easy to dry since it has a low boiling point.

PS and Co/C//PS nanocomposites characterization

The mean particles diameter or aggregates effective size (often given by the symbol Z-average) was carefully measured in a diluted solution (130 ppm Co/C in toluene) as a function of sonication conditions by dynamic light scattering (DLS) with Zetasizer Nano ZS Malvern Instrument.

Fourier transformed infrared spectroscopy (FTIR) was used to determine PS characteristic functional groups, using KBr disk (10:1 respect to sample amount). The 32 scans spectra were recorded on Nicolet iS50 FT-IR equipment from Thermo Scientific equipped with a DTGS detector.

Raman spectra were recorded in the backscattering geometry using a Renishaw Raman spectrometer. The light was focused onto the sample surface thanks to a 100 x (0.9 NA) objective with spot diameters around 1 µm. The excitation wavelength was 785 nm with a typical laser power of ~1 mW.

High resolution XPS measurements were performed using a PHI Versa Probe II spectrometer with a monochromatized Al Kα X-ray source (1486.6 eV). The electron analyzer was a concentric hemispherical analyzer, spot of 100 µm, and the electron take-off angle was θ = 45°. High-resolution spectra were recorded with a resolution of 0.5 eV.

Weight-average molecular weight was determined by gel permeation chromatography (GPC, Wyatt technology corp) equipped with Waters Styragel columns (HR4 + HR3), refractive index detector (model Waters 2414), and GPC Win software. Measurements were conducted in THF (35 °C) at a flow rate of 1 mL/min with a sample volume injection of 10 µL (20 mg of PS dissolved in 1 mL THF).

Modulated Differential Scanning Calorimetric (MDSC) was carried out on TA Q200 Instrument to study polymer and nanocomposites thermal properties. Samples were analyzed under N_2; heat/cold/heat sequence was used to erase sample thermal history (150°C/-60°C/150°C). The glass transition temperature (T_g) was determined from the second heating ramp. For a better accuracy, a low heating rate of 2 °C/min was used.

Thermogravimetric analysis (TGA) was performed on TA Instrument TGA Q500 in order to investigate the thermal stability of PS and Co/C//PS nanocomposites powders and to systematically determine the weight-fraction of nanoparticles

(wt. %) in the final products with an error of less than 1%. The samples (~ 3 mg) were heated from room temperature up to 600 °C, at 10 °C/min under N_2.

Mass-magnetization (emu/g) and hysteresis loops were also systematically measured at room temperature by Vibrating Sample Magnetometry (VSM) with Micro Sense model EZ7, applying a magnetic field up to 10.000 Oe. The mass-magnetization was calculated from the nanoparticle weight-fraction determined by TGA.

High resolution transmission electron microscopy (HR-TEM) was carried out on a 200 kV Titan FEG HR-TEM. Prior to observation samples (Co/C and Co/C//PS nanocomposites) were prepared by suspension in isopropanol followed by deposition on carbon grids (Lacy carbon film on 300 mesh Cu).

Results and discussion

Raw Co/C nanoparticles

Figure 1B shows a typical HR-TEM image at low magnification of as-received Co/C nanoparticles, showing a size distribution around 30 nm. The crystalline outer-shell observed in Figure 1C is attributed to graphene layers and the distances between layers indicate that Co/C nanoparticles are covered with approximately 6 to 8 graphene layers with a total thickness of ~ 5 nm.

Raman analysis is presented in Figure 1D. The spectrum shows one active basic E_{2g} mode corresponding to G band carbon structure at 1580 cm^{-1}, and the visible D and D' bands at 1350 and 1620 cm^{-1}, respectively, are associated with presence of sp^3 defects within the graphene sheets.[34, 35] On the spectrum, it is clearly visible that D and G bands are of similar intensities ($I_G/I_D \approx 1.25$) showing significant presence of sp^3 carbons in the sheets.[34-36] A weak band - attributed to the graphene 2D band - is observed at 2700 cm^{-1} but its low intensity reflects a disordered graphene.[35] Moreover the 2D band intensity is lower than that of G and D bands which may indicate that raw Co/C powders (*i.e.* as received) present defective graphene shells.

Finally, a small signal is also observed at approximately 700 cm^{-1} corresponding to Co_3O_4 cobalt oxide[37] indicating that within the nanoparticles batch only a small amount is already oxidized.

Co/C nanoparticles where further analyzed by HR-XPS to corroborate cobalt oxide presence as observed by Raman (Figure 1E). On the HR XPS Co $2p_{3/2}$ spectrum, a signal at 778.3 eV can be observed which is attributed to the metallic cobalt (Co^0).[38] Meanwhile, the signal of cobalt oxides expected around 780 eV was hardly detectable on the spectrum confirming that only a tiny portion of the sample is oxidized (i.e. ≤ 10 %).[38] These results show that cobalt oxides are present but to a negligible extent probably due to residual ultra-small nanoparticles that do not presented a protective graphene shell (as observed by HR-TEM).

The net saturation mass-magnetization (Ms) of Co/C powder samples was extrapolated from VSM measurements, showing a value as high as 150 emu/g, as previously reported.[12] Such high magnetization shows that the graphene shell despite not being solely constituted of sp^2 carbons protects efficiently metallic Co nanoparticles from oxidation and do not degrade magnetization. Therefore, the evidence of graphene shells around the large majority of metallic cobalt particles allows performing carbon-based surface chemistries on nanoparticles surface, such as functionalization with polymers, without risk of further massive cobalt oxidation.

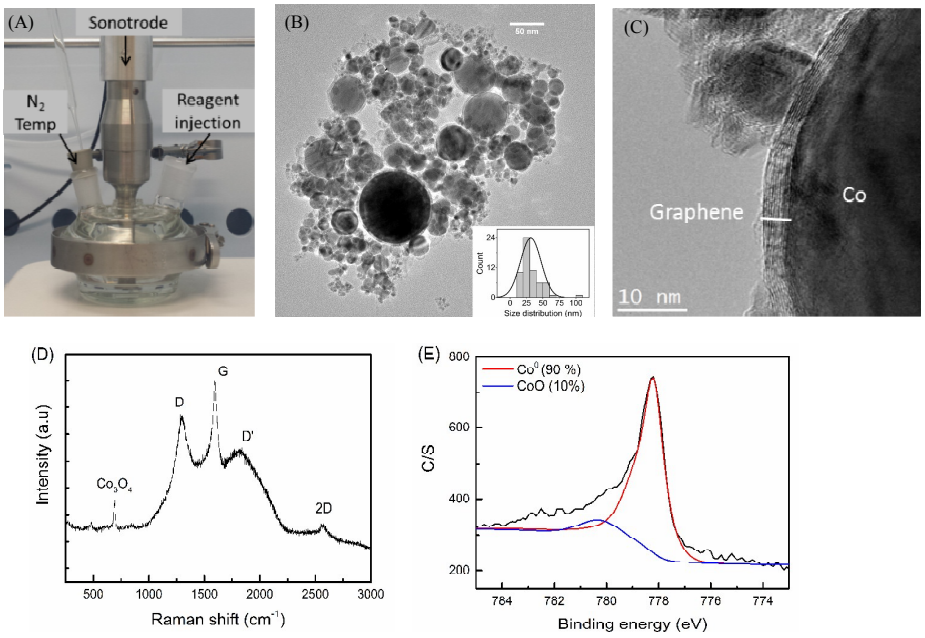

Figure 1. (A) Experimental set-up, (B) HR-TEM image at low magnification, (C) HR-TEM image at high magnification, (D)Raman spectrum, and (D) HR Co $2p_{3/2}$ XPS spectrum of raw Co/C nanoparticles.

Sonication effect on Co/C nanoparticles

First of all, Co/C nanoparticles were sonicated in toluene to avoid self-aggregation with magnetostatic interactions, due to the acoustic waves produced with high power; this energy released locally can exceed attractive energy force between nanoparticles. Indeed big agglomerates (hundreds of µm) are naturally formed principally due to magnetic dipolar interactions as such powder mainly consist of "big" ferromagnetic particles (*i.e.* 30 nm in datasheet) sustaining significant remanent magnetization (*i.e.* ~ tens of emu/g) at room temperature. To allow a better homogeneity on the final polymer/nanoparticles composite, it is important to try to get the aggregates as small as possible. For this reason, sonication steps performed under two different conditions have been tested and compared: the first one consists in combining long sonication time (30 min) with low sonication power (100 W), and the second one in short sonication time (15 min) but with high sonication power (250 W).

To get a better understanding of the sonication conditions influences on the mean particles diameter or aggregates effective size, nanoparticles dispersions were studied by dynamic light scattering (DLS) after sonication. Results showed that sonication leads to smaller aggregates of ~ 350 nm (*i.e.* ~ 7 nanoparticles) which contrasts with raw materials. However, not significant differences on the mean "particle"-size for both sonication conditions studies where found (350 ± 10 nm and 400 ± 10 nm, for 100 W and 250 W, respectively). This indicates that the critical sonication energy to fully break Co/C aggregates into individual particles is much higher (*i.e.* > 225 10^3 J, energy achieved using 250 W during 15 min).

Thermal stability of Co/C nanoparticles before and after sonication was studied by TGA (Figure 2B). First, raw Co/C nanoparticles showed a non-null weight loss (*i.e.* ~ 2 %) near 240 °C. This could imply the presence on graphene of some functional groups like hydroxyl, epoxide, and carboxyl due to the residual carbon defects, which is consistent with the D band observation in the Raman spectrum as previously explained.[39, 40] It was observed that both sonication conditions studied produce an increase on the weight loss near 240 °C. However, nanoparticles sonicated at higher power (250 W) presented higher mass loss (17 %) whereas; those sonicated at a lower power only presented a loss of 12 %. These results indicate that using high power sonication even for short time produce greater damage on the graphene shell resulting in more defects on nanoparticles surface (*i.e.* functional groups such as carbonyl, hydroxyl, etc.).

Net saturation mass-magnetization (Ms) was also studied on Co/C nanoparticles after sonication. The results are reported in Figure 2A. A decrease of 20 % (120 emu/g) to 30% (105 emu/g) on Ms was observed with respect to the initial value (*i.e.* 150 emu/g). The decrease in Ms observed can be attributed to cobalt oxide formation that can in turn indicate that during sonication the graphene shell is partially peeled-off or oxidized (*i.e.* carbonyl group formation). Indeed, it has been reported that carbonyl groups can interact with cobalt and quench spins at the surface, and as a consequence reduce the net magnetic moment.[3] Thus, early degree of cobalt oxidation (Co_3O_4 or CoO) when graphene shell starts to degrade with high energy sonication might be considered.

It is worth mentioning that even with this decrease on Ms, Co/C nanoparticles after sonication keep a much higher Ms value than those of typical magnetic oxides and more recent ferrites/graphene (*i.e.* Ferrites/C with a Ms of 20 emu/g) systems already reported in the literature (Figure 2A).[36]

Magnetic characterization is consistent with thermal stability measurements. The reduction of Ms after sonication appears as the graphene shell becomes defective as indicated by higher weight loss on TGA results and could lead to partial oxidation of Co nanoparticles. Therefore, to go further towards the synthesis of high-moment nanocomposites, sonication power and time (*i.e.* cumulative) were limited to 20% of the maximum power over 30 min.

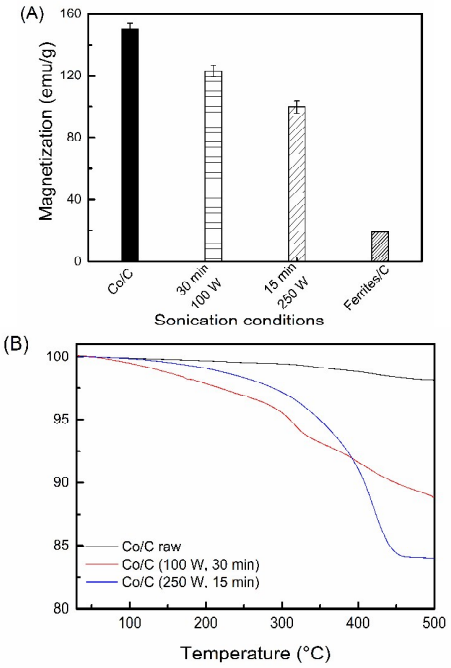

Figure 2. Influence of sonication conditions on raw Co/C nanoparticles: (A) Mass-magnetization (emu/g) comparing with Ferrites/C according to,[36] and (B) thermal stability (TGA).

Polystyrene (PS) synthesis and characterization

From previous observations, it is clear that the reaction and sonication power used to synthesize the composite should not exceed 30 min and 100 W to preserve Co/C nanoparticles integrity. So prior to Co/C//PS nanocomposites synthesis, *in situ* sonochemical polymerization of pure PS has been explored under these specific conditions (soft conditions), which differ quite a lot from what has been reported in the literature (closer to 4 h reaction time and 600 W sonication power).[28, 41]

Polystyrene synthesized by sonochemical polymerization was obtained with a yield of 12 % (± 1 %); this error indicates a

good control of the synthesis parameters and process reproducibility.

FTIR spectrum allows comparing polymer chemical structure with that of monomer (Figure 3A). As expected, PS spectrum is characterized by the disappearance of the signal at 1683 cm^{-1} corresponding to C=C double bond stretching vibration of styrene vinyl group, which confirms a successful polymerization even under these soft synthesis conditions (Figure 3B). Also, signals between 3000-2780 cm^{-1} associated to C-H bonds stretching modes became more intense due to the polymer backbone formation (sp^3 C formation). Finally, a slight shift of C-C aromatic stretching modes towards higher wavenumbers can be observed and can be explained by a lower mobility of these aromatic carbons as the polymer is formed (Figure 3B).[42]

Polymer degradation behavior was investigated by TGA; it was observed that the mass loss started at 260 °C, reaching a maximum degradation temperature at 407 °C, which is attributed to main-chain pyrolysis. Glass transition temperature determined by MDSC was observed at 74 °C which corresponds to a moderate molecular weight of 11,500 g/mol recorded by GPC,[43, 44] and which is consistent with the low reaction time employed in this work. Additionally, a low polydispersity index is reported (PI = 1.34), which indicates that the majority of polymer chains present similar molecular weight. According to literature, it is worth mentioning that obtaining a low PI with radical polymerization is a challenge, which implies a good control of all synthesis parameters.[45]

It is noteworthy that the aim of this research is not to produce high amount or high molecular PS, but to control the early beginning of the polymerization in order to form shells of few nanometers around the Co/C nanoparticles to realize close packed core-double-shell structures.

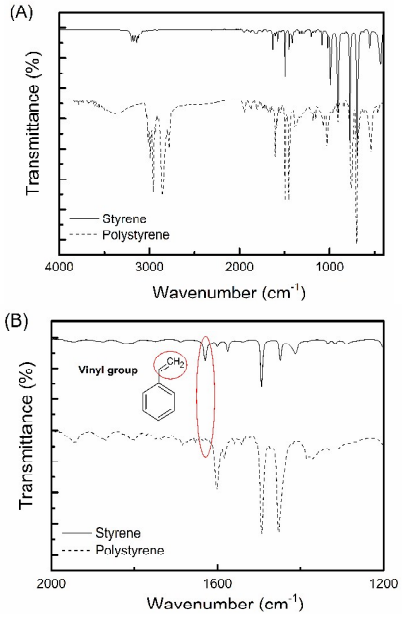

Figure 3. (A) FTIR spectrum of styrene and polystyrene after *in situ* sonochemical polymerization, (B) zoom on aromatic zone and C=C of vinyl group signal.

Co/C//PS nanocomposite synthesis and characterization

Polystyrene (PS) is a suitable polymer for hybridization with Co/C particles because it presents aromatic units and the graphene shell surrounding Co nanoparticles can interact with the polymer via π-π interactions or covalent bonding.[22]

Based on PS *in situ* sonochemical polymerization process, Co/C//PS nanocomposites were synthesized using same reaction conditions but adding Co/C nanoparticles at different reactions times. A first approach involves the addition of all main reactants at the start of the reaction (*i.e.* t = 0 min) to enable the polymer growth step by step on nanoparticles surface; such method is defined in the literature as a "grafting from" method.[33] In the second approach, the synthesis procedure consists in adding Co/C nanoparticles 15 min after the reaction started (*i.e.* t = 15 min). Under these conditions, it is expected that the nanoparticles react with the radicals of the growing polymer chains and quench (*i.e.* stop) PS polymerization leading to the pre-formed polymer being grafted to the nanoparticles surface. In contrast to the first case, this second process is known as a "grafting to" method.[33] In both cases, it is expected that the polymer will be covalently grafted to the graphene on nanoparticles surface, which allows obtaining more homogeneous and reliable nanocomposites.[23, 46]

When nanoparticles are added at 0 min no significant difference was observed compared to the yield achieved in PS synthesis (*i.e.* ~ 12 %). In contrast, adding them at 15 min leads to 9 % of yield (Figure 4A). So adding Co/C nanoparticles at different reaction times has a real impact on reaction yields. This could indicate that adding the nanoparticles after 15 min after starting the reaction PS polymerization is quenched and as a consequence the amount of polymer formed is lower. It is worth commenting that in both synthesis methods polymer chains might also grow ungrafted (*i.e.* free-PS matrix) and grafted to nanoparticles surface.

Co/C//PS nanocomposites were precipitated in methanol to remove unreacted species (*i.e.* monomer or initiator). After this process dry nanocomposites were studied by TGA. The results are reported in Figure 4B. This technique not only allows studying thermal stability, but also quantifies Co/C nanoparticles amount (*i.e.* wt. %) originally presents in the nanocomposite. Adding Co/C at different reaction times lead to different weight fractions in the nanocomposites. According to the weight loss measured by TGA, one concludes that Co/C//PS nanocomposites synthesized at 0 min and 15 min contained 17 wt. % and 33 wt. % of Co/C, respectively. This result is related to polymerization yields obtained; in both synthesis PS amount synthetized is not the same, and as a consequence the ratio polymer/nanoparticles changes. Therefore, one might consider that adding nanoparticles at 15 min during *in situ* polymerization produces less amount of PS which leads to higher wt. % of Co/C, as was observed in the results.

Concerning Co/C//PS thermal stability, Figure 4C clearly showed that both initial and maximum degradation temperatures have shifted towards higher values compared to PS alone. These changes in degradation temperature indicate

that the composites presented higher thermal stability. Adding nanoparticles into a polymeric matrix that can form covalent bond with the polymer, might reduce polymer chain mobility and as a consequence all polymer degradation process is delayed, enhancing thermal resistance of the final nanocomposite.[32]

One way to corroborate a possible covalent interaction between PS and Co/C nanoparticles is to closely study changes in glass transition temperature (T_g) from the different final products. For this reason, modulated differential scanning calorimetry (MDSC) studies were carried out with PS and Co/C//PS nanocomposites. Results are presented in Figure 4D. As a clear observation, nanocomposites exhibit higher T_g than PS alone (*i.e.* 84-86°C vs. 74°C, respectively). According to [32, 47, 48] T_g increases as polymer chains mobility is reduced and density is increased when covalent bonds between polymer and nanoparticles take place. Thus, T_g gives indication on the covalent bonding between the polymer and the graphene shell. To prove this, Co/C//PS powder was further washed with chloroform to remove all free-polymer, not covalently grafted to nanoparticles surface.

The final purified powders were analyzed by TGA to quantify PS amount covalently immobilized, results are shown in Figure 5A (labelled as Co/C//PS without free PS). Also, DLS measures were carried out on Co/C//PS_0min without free PS to study the size distribution of synthesize double core shell nanocomposite.

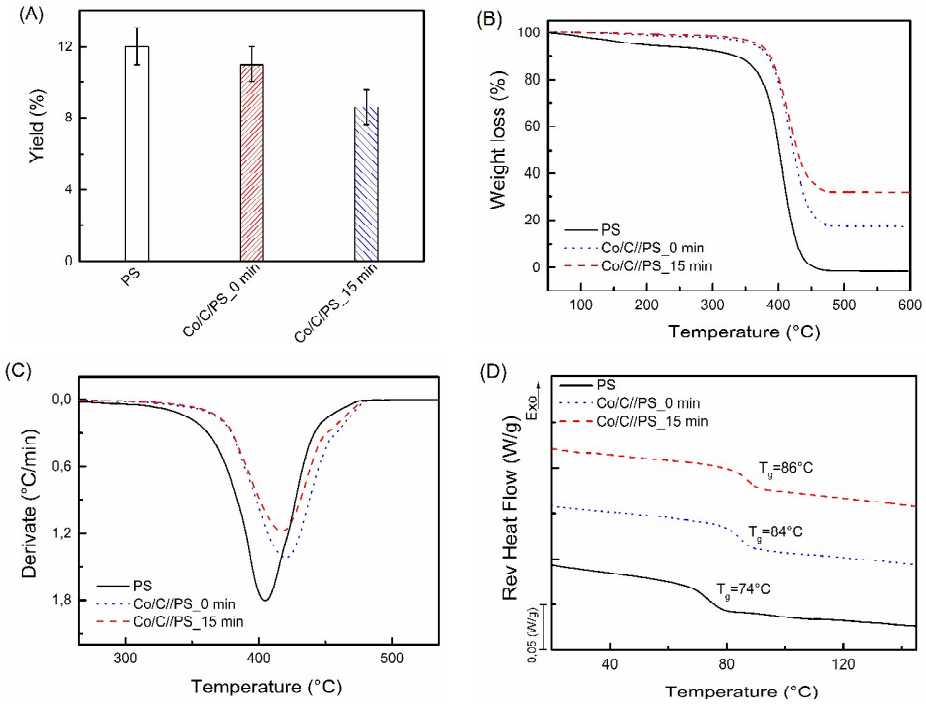

Figure 4. PS and Co/C//PS nanocomposites: (A) synthesis yield, (B) TGA thermogram, (C) TGA first derivate, (D) MDSC thermogram.

Significant differences were observed in PS amount covalently grafted. Nanocomposite synthetized by "grafting from" (t = 0 min) process presented a 35 % PS covalent grafted, meanwhile, by "grafting to" (t = 15 min) process only 6 % of the polymer synthetized was successfully covalently bounded. This could be attributed to the fact that 15 min after starting the reaction the amount of radicals available to react with nanoparticles surface is lower, because the majority has already reacted with monomer molecules to form polymer chains. Also, nanoparticles access to the growing radical polymer chain could be limited by steric hindrance produced by the spherical polymer structure. For these reasons, adding Co/C nanoparticles at the beginning of the reaction promotes more covalent interaction between polymer and nanoparticles. These results demonstrated that nanocomposites synthesized by *in situ* sonochemical polymerization (*i.e.* grafting to or grafting from) presented covalent bonds between polymer and nanoparticles surfaces.

Synthesized double core shell nanoparticles (t = 0 min) were studied by light scattering (DLS) showing a size distribution of 700 ± 100 nm. When this value is compared with initial particle size distribution (after sonication 350 ± 10 nm) a significant increase it is observed, this could be attributed to the polymer shell that is covalently bound to the nanoparticles surface, increasing the volume of the final agglomerates, consisting of approximately 20 Co/C nanoparticles.

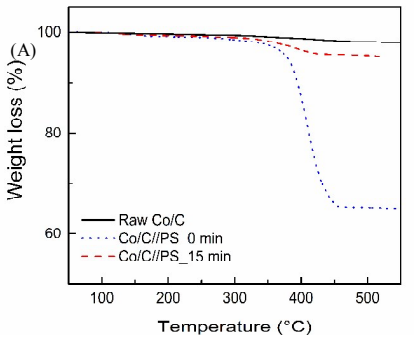

Figure 5. Thermograms of Co/C//PS nanocomposites without free-PS.

According to these observations and previous studies known from literature [23, 32, 41, 47] a possible reactions scheme is proposed in Figure 6, where is illustrated the interaction between PS and Co/C taking place when nanoparticles are introduced at the beginning of the reaction (*i.e.* "grafting from") and during the reaction (*i.e.* "grafting to").

Polystyrene sonochemical polymerization starts with a radical initiation reaction step between AIBN (initiator radicals) and styrene molecules (monomer radicals, also formed during sonication), followed by a propagation process that allowed polymer chain growth. Figure 6 shows a schematic classic radical PS polymerization process.

Co/C//PS nanocomposites synthesis relates to two possible grafting mechanisms, depending at what time Co/C nanoparticles are added into the polymerization medium. When they are added at the early beginning of polymerization, known as grafting from process, AIBN radicals are able to attack and open π-bonds of conjugated carbonaceous backbones. Such mechanisms have been proposed for AIBN and MWCNT system,[20] which can be extrapolated to AIBN and Co/C system since MWCNT and graphene sheets present similar chemical structure (sp^2 carbon atoms). Reaction between AIBN and Co/C nanoparticles are promoted by cavitation bubbles – caused by high or moderate power sonication – enabling the vibration of molecules and nanoparticles, enhancing their reaction and promoting radical initiation on graphene layers. The radical polymerization initiated on styrene monomer resulting in covalent bounding with the graphene surface. The reaction propagates further to other radicals monomers in solution to develop polymer chains of PS. Also, a portion of AIBN radical can react with styrene molecule in solution resulting in a residual polymeric matrix of unbounded polymer (free-PS) surrounding Co/C//PS nanocomposites.

In contrast, when Co/C nanoparticles are introduced 15 min after starting the reaction ("Grafting to" method) they could covalently bond to the radical polymer chains that have been formed during the first 15 min of the reaction. It is worth mentioning, that if some radical terminations of the polymer chains and nanoparticles do not react together, the polymer propagation process continues, as classic polymerization process and a free-PS matrix surrounding Co/C nanoparticles is obtained like for "grafting from" mechanism.

One notes, that whatever the mechanism, free-PS may be kept to form a solid film of Co/C//PS being self-encapsulated within the free-polymer matrix or washed to keep only homogeneously dispersed core-double-shell Co/C//PS product.

Raman spectroscopy was performed on Co/C//PS nanocomposites (Figure 7A). The spectrum shows peaks of polystyrene confirming polymer formation. However those corresponding to graphene shell (*i.e.* 1580 cm^{-1} and 1350 cm^{-1}) are no longer observed. This could be due to a shielding of these signals by those of PS or be a disappearance or a decrease in intensity of these signals due to an amorphization of the graphene shell. If graphene peaks disappears, it confirms the covalent functionalization (sp^2 carbons converted into sp^3) that is already corroborated by TGA analysis of nanocomposites without free-PS (Figure 5). Such observation gives a hint for graphene layer amorphization upon polymer immobilization. Also, the Raman spectra peaks assigned to A_{1g} (690 cm^{-1}) vibration mode of Co_3O_4 crystalline phase is present in both the composite.[37, 49] This may indicate that residual ultra-small oxidized Co nanoparticles, already observed in raw nanoparticles, are present in the final nanocomposite. This peak is more intense on the composite synthesized by "grafting from" method than those obtained using the "grafting to" method. Such result are in line with the TGA observations recorded on nanocomposites without free-PS that showed that the nanocomposite obtained by the "grafting" from method are more grafted than those synthesized by the "grafting to" method, and as a consequence the probability of oxidation is higher in the first case.

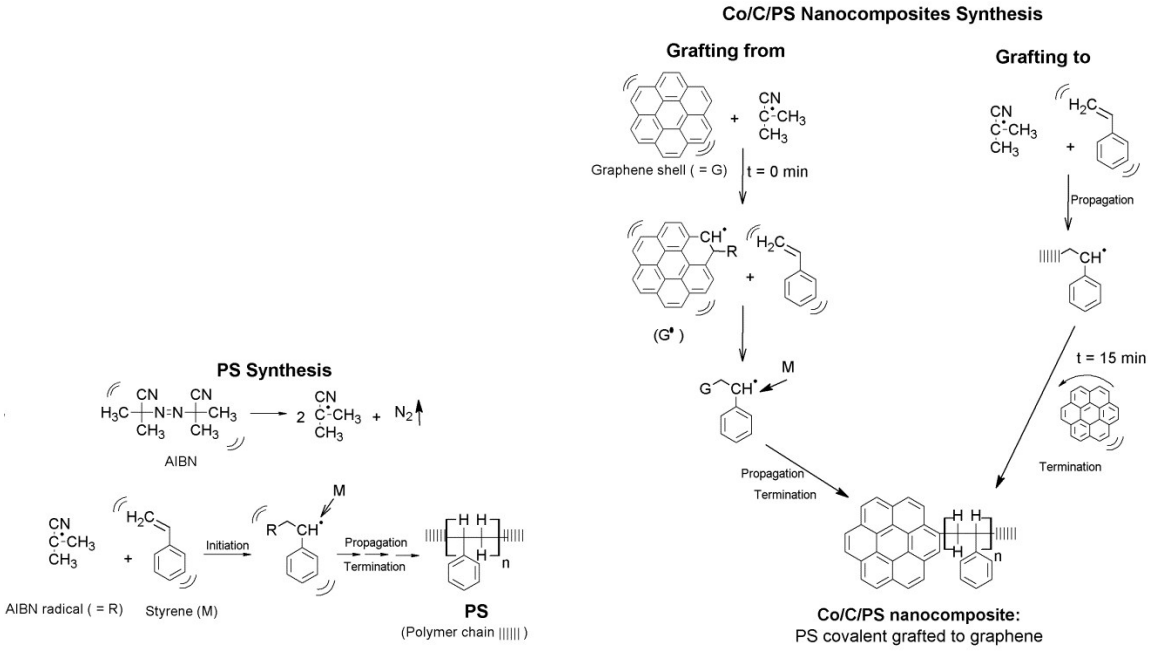

Figure 6. Schematic classical radical PS polymerization and possible reaction schemes of Co/C//PS *in situ* polymerization process.

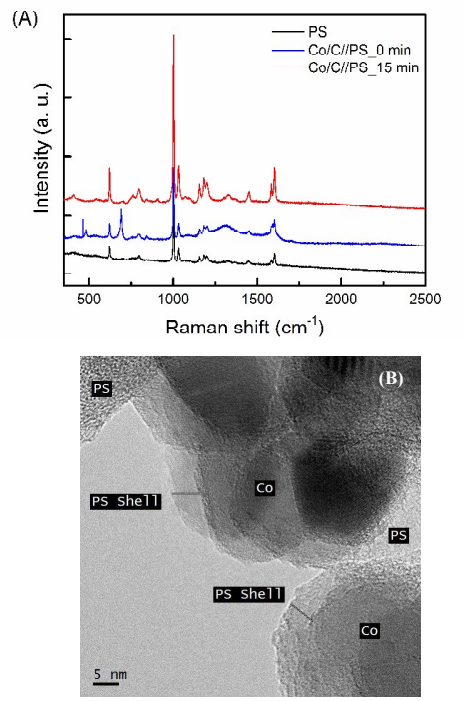

Figure 7. (A) PS and Co/C//PS nanocomposites Raman spectra, (B) HR-TEM image of Co/C//PS_15 min.

To confirm the absence of the graphene layers, Co/C//PS nanocomposite (synthesized by grafting from method t = 15 min) was closely analyzed by HR-TEM (Figure 7B). In this picture graphene layers are hardly observed, proving a partial or total amorphization during PS synthesis process. Indeed, it is known from the literature that AIBN radicals are able to open π-bond on MWCNT structure inducing structural damages leading to carbon amorphization.[47] As Co/C and MWCNT have the same carbonaceous surface structure and the used chemistries are close, similar damages seems to occur here.

HR-TEM image also reveals that, Co/C nanoparticles are embedded into polymeric matrix (*i.e.* free-PS) and that a thin outer polymer shell is surrounding nanoparticles or small aggregates consisting of few tens of nanoparticles. As a major result, the thickness of the covalent grafted-PS shell is of approximately 5.5 ± 0.2 nm. It is worth mentioning, that this polymer shell presents a similar thickness than initial graphene layers, allowing protecting cobalt nanoparticle from complete or partial oxidation.

Saturation mass-magnetization of Co/C//PS nanocomposites was evaluated in both composites (t = 0min and 15 min). The results are shown in Figure 8. Nanocomposites with free-PS exhibit lower Ms as the excess of polymer (*i.e.* matrix) is taken into account in the mass-magnetization evaluation. Conversely, samples without free-PS (*i.e.* purified) possess higher Ms values as they eventually contain less amount of polymer. Now, the difference over Ms between the nanocomposites without free-PS is an indication of how much polymer successfully covalently bound to Co/C nanoparticles, depending on the synthesis method employed. Samples obtained by "grafting from" method (Co/C//PS_0 min) show lower Ms because higher amount of PS is covalently grafted on graphene shell (*i.e.* 35 % corroborated by TGA). On the contrary, samples obtained following "grafting to" method (Co/C//PS_15 min) present higher Ms value because less amount of PS (*i.e.* 16 %) has been grafted to nanoparticles surface (*i.e.* Co/C weight fraction is higher).

Knowing the exact weight fraction of grafted PS - determined by TGA - mass-magnetization of these nanocomposites without

free PS (30 emu/g for Co/C//PS_0 min and 45 emu/g for Co/C//PS_15 min) are converted into equivalent net mass-magnetization of the Co/C particles composing the samples. Calculations lead to ~ 49 emu/g (Co/C//PS_0 min) and 45 emu/g (Co/C//PS_15 min), without significant differences between the synthesis method employed and the amount of PS covalent grafted. This decrease of the Ms value -compared to that obtained for raw Co/C nanoparticles (*i.e.* 115 emu/g)- could be attributed to the partial degradation of the graphene shell after covalent grafting, as hinted the TEM images of Co/C//PS_0 min after removing free PS (Figure. 9), where only few graphene layers are observed (*i.e.* 3 layers instead of 8 presented on raw Co/C nanoparticles). This result confirmed partial amorphization of graphene layers during nanocomposites synthesis.

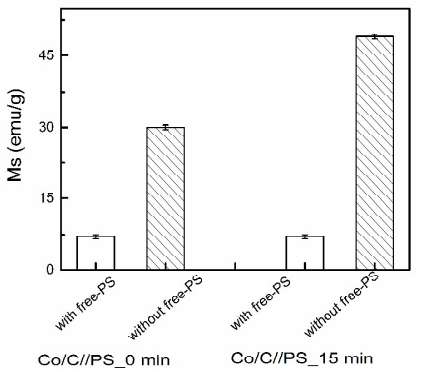

Figure 8. Comparison of mass-magnetization (M_s) of Co/C//PS with (not purified) and without free-PS (purified).

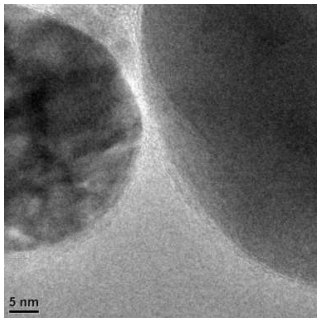

Figure 9. HR-TEM image of Co/C//PS_0 min without free-PS.

Despite these differences between the saturation magnetization of nanocrystals and that of the bulk it is worth underlining that Ms values obtained for Co/C//PS nanocomposites exceed those of existing systems, for examples: Fe_3O_4/C core-shell composite with a Ms of 20 emu/g,[36] Ni/C with 32 emu/g,[13] Fe/copolymer double core-shell (*i.e.* core of 30 nm and copolymer shell of 5 nm) with a Ms of ~ 12 emu/g.[50]

Another important discrimination point between the two synthesis path employed is the tradeoff between a superior mass-magnetization with weak covalent bond (Co/C//PS_15 min) and superior chemical stability and potential mechanical resistance achieved with strong covalent bonds (Co/C//PS_0 min). Nanocomposites synthesis will be selected in function of the final application. *In situ* sonochemical polymerization also gives the opportunity to produce simultaneously the polymer matrix (*i.e.* free-PS) that can be kept or not (*i.e.* after removing free-PS with chloroform). In the first case, it allows forming a ready to use solid material, for example here a small disk, being self-embedded within the polymeric matrix (Figure 10A and 10C). In the second case, it produces a purified powder of core double-shell Co/C//PS particles that can be used to prepare another solution. Indeed, it can be mixed with a subsidiary polymer (*i.e.* PS with higher molecular weight) for better mechanical cohesion and promoting film formation for example (Figure 10B).

Going beyond, both types of nanocomposites produced in this work are useful for the production of self-supporting flexible magnets with low temperature molding or magnetic films on substrate with spin coating. In that case, volume-magnetization (*i.e.* emu/cm^3) has more meaning for applications. Then it depends on the volume fraction of Co/C//PS particles embedded in the subsidiary polymer. The idea of maximum volume fraction - or percolation threshold - is essential with Type C nanocomposites where properties are controlled by volume occupation. With core-shell structures there is a tradeoff between the shell thickness and the particle size as it determines the percolation threshold. For example, with a core of 50 nm and a graphene shell of 5 nm it decreases down to 45 vol.%, and decreases even more to 27 vol.% when a PS shell of 5 nm is present in the nanocomposite.[48]

For the microelectronics and microsystems community, the achievement of processable films of high moment magnetic nanocomposite (*i.e.* no conductive) with high percolation threshold is a decisive step towards further applications beyond usual solid state devices. This would not be possible without high mechanical cohesion. We conclude that promoting covalent bonds with Co/C and PS, as recently shown with hydrogels for magnetic elastomeric materials for biomechanic application,[24] is decisive.

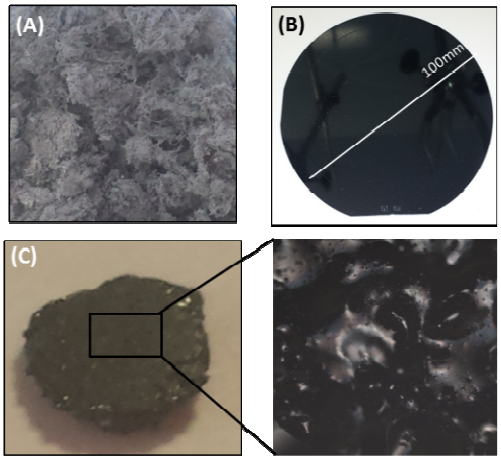

Figure 10. A) Co/C//PS nanocomposite powder, B) film of Co/C//PS (without free-PS) mixed with 2nd polymer deposited by spin coating on silicon substrate, and C) disk of melted and compressed Co/C//PS powder with free-PS.

Conclusion

Physico-chemical properties of magnetic nanocomposites cobalt/graphene/polystyrene (Co/C//PS) with a novel core double-shell structure were reported. *In situ* sonochemical polymerization technique was used starting from commercial Co/C nanoparticles and successfully lead to gram-scaled production of processable materials. Co/C//PS nanocomposites showed improved thermal properties in contrast to neat PS with evidence of covalent bonds between the polymer and the graphene. Depending on nanoparticles addition time in the reaction medium, two surface reaction mechanisms were proposed, namely; "grafting to" and "grafting from". HR-TEM observations revealed polymer shells of about 4 to 5 nm perfectly covering Co/C nanoparticles or at least small aggregates. Graphene layers were reduced after sonochemical polymerization indicating partial carbon amorphization with the promotion of covalent interactions. As a consequence a reduction of the net moment of Co was observed but usually there is much larger difference between the saturation magnetization of nanoparticles and that of the bulk. Finally, we report a remarkable high saturation mass-magnetization (*i.e.* up ~ 49 emu/g for 94 % wt.) with purified Co/C//PS with covalent grafting. Evidences of satisfying mechanical cohesion are shown with a sample of hot pressed disk and that of a spin coated film. Thereby, it is concluded that *in situ* sonochemical polymerization plays a key role in producing processable artificial high moment magnetic materials which is a decisive step for further applications beyond usual solid state devices.

Acknowledgements

The authors would like to thank the Nanoscience Transversal and Chimtronique Programs of the CEA for their financial support. This work has been performed with the technological support of the Minatec Nanocharacterization Platform (PFNC) of Grenoble. The involvement of H. Okuno - for TEM images recording and analyzing - and of D. Rouchon - for Raman measurements analysis - is finally greatly acknowledge.

Notes and references

[a] CEA, LETI, MINATEC Campus, Grenoble, France.
[b] LTM-CNRS-UJF, CEA, LETI, MINATEC Campus, Grenoble, France.
[c] Univ. Grenoble Alpes, INAC-SCIB, F-38000 Grenoble, France.

1. C. B. Murray, S. Sun, H. Doyle and T. Betley, *MRS Bulletin* **2001**, 26
2. D. L. Leslie-Pelecky and R. D. Rieke, *Chemistry of Materials* **1996**, 8
3. D. A. van Leeuwen, J. M. van Ruitenbeek, L. J. de Jongh, A. Ceriotti, G. Pacchioni, O. D. Häberlen and N. Rösch, *Physical Review Letters* **1994**, 73
4. S. Sun and C. B. Murray, *Journal of Applied Physics* **1999**, 85
5. N. Matoussevitch, A. Gorschinski, W. Habicht, J. Bolle, E. Dinjus, H. Bönnemann and S. Behrens, *Journal of Magnetism and Magnetic Materials* **2007**, 311
6. T. Hayashi, S. Hirono, M. Tomita and S. Umemura, *Nature* **1996**, 381
7. K. S. Kumar, V. B. Kumar and P. Paik, *Journal of Nanoparticles* **2013**, 2013, 1.
8. G. Qiu, Q. Wang, C. Wang, W. Lau and Y. Guo, *Ultrasonics Sonochemistry* **2007**, 14, 55.
9. J.-H. Lee, M. A. Mahmoud, V. B. Sitterle, J. J. Sitterle and J. C. Meredith, *Chemistry of Materials* **2009**, 21, 5654.
10. S. Xing, L. H. Tan, M. Yang, M. Pan, Y. Lv, Q. Tang, Y. Yang and H. Chen, *Journal of Materials Chemistry* **2009**, 19, 3286.
11. E. K. Athanassiou, R. N. Grass and W. J. Stark, *Nanotechnology* **2006**, 17
12. R. N. Grass and W. J. Stark, *Journal of Materials Chemistry* **2006**, 16, 1825.
13. A. A. El-Gendy, E. M. M. Ibrahim, V. O. Khavrus, Y. Krupskaya, S. Hampel, A. Leonhardt, B. Büchner and R. Klingeler, *Carbon* **2009**, 47
14. V. Georgakilas, M. Otyepka, A. B. Bourlinos, V. Chandra, N. Kim, K. C. Kemp, P. Hobza, R. Zboril and K. S. Kim, *Chemical Reviews* **2012**, 112, 6156.
15. A. S. Patole, S. P. Patole, H. Kang, J.-B. Yoo, T.-H. Kim and J.-H. Ahn, *Journal of Colloid and Interface Science* **2010**, 350, 530.
16. R. K. Layek and A. K. Nandi, *Polymer* **2013**, 54, 5087.
17. Y. Lu, Y. Yin, B. T. Mayers and Y. Xia, *Nano Letters* **2002**, 2
18. M. Niederberger, *Accounts of Chemical Research* **2007**, 40
19. A. K. S. M. Nelo, V. K. Palukuru, J. Juuti, H. Jantunen, *Progress In Electromagnetics Research* **2010**, 253.
20. S.-M. Yuen, C.-C. M. Ma, C.-Y. Chuang, K.-C. Yu, S.-Y. Wu, C.-C. Yang and M.-H. Wei, *Composites Science and Technology* **2008**, 68, 963.
21. W. Zheng, F. Gao and H. Gu, *Journal of Magnetism and Magnetic Materials* **2005**, 288
22. K. S. Khuong, Jones, Walter H., Pryor, William A., Houk, K. N., *Journal of the American Chemical Society* **2005**, 127, 1265.
23. H. Xu and K. S. Suslick, *Journal of the American Chemical Society* **2011**, 133
24. R. Fuhrer, E. K. Athanassiou, N. A. Luechinger and W. J. Stark, *Small* **2009**, 5
25. Y. Kojima, S. Koda and H. Nomura, *Ultrasonics Sonochemistry* **2001**, 8, 75.
26. B.-J. P. Ke Zhang, Fei-Fei Fan, Hyoung Jin Choi *Molecules* **2009**, 14, 2095.
27. A. Gedanken, *Ultrasonics Sonochemistry* **2004**, 11, 47.
28. H. J. Choi, K. Zhang and J. Y. Lim, *Journal of Nanoscience and Nanotechnology* **2007**, 7, 3400.
29. F. Beckert, A. M. Rostas, R. Thomann, S. Weber, E. Schleicher, C. Friedrich and R. Mülhaupt, *Macromolecules* **2013**, 46, 5488.
30. W.-P. Wang and C.-Y. Pan, *Polymer* **2004**, 45
31. H. Roghani-Mamaqani, V. Haddadi-Asl, K. Khezri, E. Zeinali and M. Salami-Kalajahi, *J Polym Res* **2013**, 21, 333.
32. H. Hu, X. Wang, J. Wang, L. Wan, F. Liu, H. Zheng, R. Chen and C. Xu, *Chemical Physics Letters* **2010**, 484, 247.
33. S. Minko, in *Polymer Surfaces and Interfaces*, ed. M. Stamm, Springer Berlin Heidelberg, 2008, DOI: 10.1007/978-3-540-73865-7_11, ch. 11, pp. 215-234.
34. M. Fang, K. Wang, H. Lu, Y. Yang and S. Nutt, *Journal of Materials Chemistry* **2009**, 19

35. V. Singh, D. Joung, L. Zhai, S. Das, S. I. Khondaker and S. Seal, *Progress in Materials Science* **2011**, 56
36. Z. L. Tieshi Wang, Mingming Lu, Bo Wen, Qiuyun Ouyang, Yujin Chen, Chunling Zhu, Peng Gao, Chunyan Li, Maosheng Cao and Lihong Qi, *Journal of Applied Physics* **2013**, 113, 024314
37. C.-W. Tang, C.-B. Wang and S.-H. Chien, *Thermochimica Acta* **2008**, 473, 68.
38. M. C. Biesinger, B. P. Payne, A. P. Grosvenor, L. W. M. Lau, A. R. Gerson and R. S. C. Smart, *Applied Surface Science* **2011**, 257
39. H.-K. Jeong, Y. P. Lee, M. H. Jin, E. S. Kim, J. J. Bae and Y. H. Lee, *Chemical Physics Letters* **2009**, 470, 255.
40. Y. P. L. Hae-Kyung Jeong , Rob J. W. E. Lahaye , Min-Ho Park , Kay Hyeok An , Ick Jun Kim , Cheol-Woong Yang ,Chong Yun Park , Rodney S. Ruoff , and Young Hee Lee, *Journal of the American Chemical Society* **2008**, 130
41. S. Kim, H. Choi and S. Hong, *Colloid Polym Sci* **2007**, 285
42. C. Y. L. a. S. KRIMM, *Journal of Polymer Science* **1958**, 27, 241.
43. T. G. Fox and P. J. Flory, *Journal of Polymer Science* **1954**, 14
44. P. G. Santangelo, Roland, C. M., *Macromolecules* **1998**, 31, 4581.
45. M. F. Cunningham, *Progress in Polymer Science* **2008**, 33
46. Z. Spitalsky, D. Tasis, K. Papagelis and C. Galiotis, *Progress in Polymer Science* **2010**, 35, 357.
47. M. A. Pantoja-Castro, J. F. Pérez-Robles, H. González-Rodríguez, Y. Vorobiev-Vasilievitch, H. V. Martínez-Tejada and C. Velasco-Santos, *Materials Chemistry and Physics* **2013**, 140, 458.
48. T. Hanemann and D. V. Szabó, *Materials* **2010**, 3
49. J. Llorca, P. Ramírez de la Piscina, J.-A. Dalmon and N. Homs, *Chemistry of Materials* **2004**, 16, 3573.
50. N. A. D. Burke, H. D. H. Stöver and F. P. Dawson, *Chemistry of Materials* **2002**, 14

